International Journal of Pharmaceutics 423 (2012) 55–62

Contents lists available at ScienceDirect

International Journal of Pharmaceutics

journal homepage: www.elsevier.com/locate/ijpharm

Administration-dependent efficacy of ferrociphenol lipid nanocapsules for the treatment of intracranial 9L rat gliosarcoma

Ngoc Trinh Huynh[a,b], Catherine Passirani[a,b,*], Emilie Allard-Vannier[a,b], Laurent Lemaire[a,b], Jerome Roux[c], Emmanuel Garcion[a,b], Anne Vessieres[d], Jean-Pierre Benoit[a,b]

[a] LUNAM Université, Ingénierie de la Vectorisation Particulaire, F-49933 Angers, France
[b] INSERM U646, F-49933 Angers, France
[c] Service Commun d'Animalerie Hospitalo-Universitaire (SCAHU), Angers F-49100, France
[d] CNRS, UMR 7223, Ecole Nationale Supérieure de Chimie de Paris, F-75231, France

ARTICLE INFO

Article history:
Received 11 February 2011
Received in revised form 8 April 2011
Accepted 15 April 2011
Available online 21 April 2011

Keywords:
Brain tumour
DSPE-mPEG2000
Convection-enhanced delivery (CED)
Intra-carotid injection
PEGylated nanoparticles

ABSTRACT

The anti-tumour effect of ferrociphenol (FcdiOH)-loaded lipid nanocapsules (LNCs), with or without a DSPE-mPEG2000 coating, was evaluated on an orthotopic gliosarcoma model after administration by convection-enhanced delivery (CED) technique or by intra-carotid injection. No toxicity was observed by MRI nor by MRS in healthy rats receiving a CED injection of FcdiOH-LNCs (60 μL, 0.36 mg of FcdiOH/rat) when the pH and osmolarity had been adjusted to physiological values prior to injection. At this dose, the treatment by CED with FcdiOH-LNCs significantly increased the survival time of tumour-bearing rats in comparison with an untreated group (28.5 days vs 25 days, $P = 0.0009$) whereas DSPE-mPEG2000–FcdiOH-LNCs did not exhibit any efficacy with a median survival time of 24 days. After intra-carotid injection (400 μL, 2.4 mg of FcdiOH/rat), hyperosmolar DSPE-mPEG2000–FcdiOH-LNCs markedly increased the median survival time (up to 30 days, $P = 0.0008$) as compared to the control (20%). This was strengthened by their evidenced accumulation in the tumour zone and by the measure of the fluorescent brain surface obtained on brain slides for these DiI-labelled LNCs, being 3-fold higher than for the control. These results demonstrated that, depending upon the administration route used, the characteristics of LNC suspensions had to be carefully adapted.

1. Introduction

The incidence rate of brain tumours has increased remarkably and tended to be higher in developed, industrialised countries (Parkin et al., 2005). Among the various types of brain tumour, glioblastomas represent the most prevalent and malignant gliomas in adults (grade IV classified by the World Health Organization – WHO) (Louis et al., 2007). In spite of numerous, notable advances in diagnosis techniques and also in multimodal therapy regimes including surgical resection followed by radiotherapy and adjuvant chemotherapy (Stupp et al., 2005), the survival prognosis always remains unfavourable, most patients dying within 2 years after diagnosis (Grossman and Batara, 2004). In terms of chemotherapy, the effort in drug discovery and development has been limited due to the obstacle of the blood–brain barrier (BBB) which prevents the delivery of drugs to the central nervous system (CNS) by means of a systemic injection (Pardridge, 2005; Segal, 2000).

Over the last decades, the technique of drug delivery to the brain by convection-enhanced delivery (CED) has provided an interesting tool of administration for brain cancer chemotherapy (Bobo et al., 1994). This technique consists in the continuous injection of a therapeutic fluid under positive pressure. CED injection allows a local administration of large doses of infusate which is mainly distributed within the interstitial spaces of tissues by a gradient of pressure that enhances constitutive intracellular medium convection (Allard et al., 2009b). Indeed, by using lipid nanocapsules (LNCs) which are characterised by a hybrid structure between polymer nanocapsules and liposomes (Huynh et al., 2009), a previous study demonstrated the wide distribution area throughout the injected hemisphere (Vinchon-Petit et al., 2010). Homogeneity of Nile Red-labelled LNCs around the injection site was observed for 24 h following a CED injection into the brain of healthy rats. Moreover, on 6-day-old 9L tumour-bearing rats, Nile Red-labelled LNCs fully covered the tumour zone and were found in the cytoplasm of tumour cells.

Recently, a new series of organometallic tamoxifen derivatives have been developed by adding a potentially cytostatic ferrocene moiety to the tamoxifen skeleton (Jaouen et al., 2000a; Top et al., 2003; Vessieres et al., 2005). The mechanism of these ferrocene

* Corresponding author at: LUNAM Université, Ingénierie de la Vectorisation Particulaire, F-49933 Angers, France. Tel.: +33 244 688534; fax: +33 244 688546.
E-mail address: catherine.passirani@univ-angers.fr (C. Passirani).

0378-5173/$ – see front matter © 2011 Elsevier B.V. All rights reserved.
doi:10.1016/j.ijpharm.2011.04.037

derivatives is believed to act as an intramolecular catalyst for the oxidation of the phenol group in mild conditions, leading to the production of quinone methides which are strongly toxic (Hillard et al., 2005). These last compounds may interact with macromolecules such as glutathione, DNA and certain proteins leading to the tumour cell's death by accelerated senescence (Vessieres et al., 2005). Among these derivatives, the compound 2-ferrocenyl-1,1-bis(4-hydroxyphenyl)-but-1-ene, or ferrociphenol compound (FcdiOH) has proved *in vitro* to be an effective cytostatic compound (IC_{50} = 0.7 μM on MCF-7 hormone-dependent and IC_{50} = 0.44 μM on MDA-MB231 hormone-independent breast cancer cell lines) (Vessieres et al., 2005). FcdiOH loaded into the oily core of LNCs (FcdiOH-LNCs) at high concentrations (6.5 mg/g, 2% dried weight) showed remarkable antitumour effects in a subcutaneous, 9L gliosarcoma model after an intra-tumoural injection (Allard et al., 2008b). FcdiOH-LNCs improved the survival time of rats in an intracranially implanted 9L gliosarcoma model when administered by CED in a dose-dependent manner (Allard et al., 2009a). Moreover, a synergistic effect was also observed between chemotherapy with FcdiOH-LNCs and external irradiation revealing the radiosensitive properties of FcdiOH (Allard et al., 2010). However, some neuronal side effects in the injected hemisphere observed in long-term survivors receiving the highest LNC suspension concentration have been reported previously (Allard et al., 2008a).

This study aimed at evaluating the impact of FcdiOH-LNCs on the rat brain after CED administration by magnetic resonance imaging before and after some adjustments assessed as needed for effective and safe administration. Furthermore, the antitumour efficacy of these modified FcdiOH-LNCs delivered by CED technique on an intracranial gliosarcoma rat model was evaluated. As an alternative route of drug administration to the brain (Alam et al., 2010), intra-carotid injection of FcdiOH-LNCs through the carotid artery was investigated in order to increase the volume of drug administered. Moreover, the efficacy of FcdiOH-LNCs coated with longer chains of polyethylene glycol (PEG) was also assessed in order to test the effect of long-circulating properties brought by this polymer (Morille et al., 2010).

2. Materials and methods

2.1. Materials

Ferrociphenol, abbreviated as FcdiOH, was prepared by a McMurry coupling reaction (Jaouen et al., 2000b). The lipophilic Labrafac® CC (caprylic-capric acid triglycerides) was purchased from Gattefosse S.A. (Saint-Priest, France). Lipoïd® S75-3 (soybean lecithin at 69% of phosphatidylcholine) came from Lipoïd Gmbh (Ludwigshafen, Germany); Solutol® HS15 (a mixture of free polyethylene glycol 660 and polyethylene glycol 660 hydroxystearate) from BASF (Ludwigshafen, Germany) and NaCl from Prolabo (Fontenay-sous-bois, France). Deionised water was acquired from a Milli-Q plus system (Millipore, Paris, France) and sterile water from Cooper (Melun, France). 1,2-Distearoyl-sn-glycero-3-phospho-ethanolamine-N-[methoxy-(polyethylene glycol)-2000] (DSPE-mPEG2000) (mean molecular weight (MMW) = 2805 g/mol) was kindly provided by Avanti Polar Lipids (Alabaster, USA). 1,10-Dioctadecyl-3,3,30,30-tetramethylindocarbocyanine perchlorate (DiI) was obtained from Introgen (Cergy, Pontoise, France).

2.2. Preparation of the LNCs

2.2.1. Anticancer agent-loaded LNCs

In this study, fifty-nanometer diameter LNCs, whose formulation is based on the phase-inversion phenomenon of a microemulsion, were prepared in conformity with the described procedure (Heurtault et al., 2002). Briefly, the preparation process involved 2 steps. Step I consisted of mixing all the components (Solutol® HS15 (17% w/w), Lipoid® (1.5% w/w), Labrafac® (20% w/w), NaCl (1.75% w/w) and water (59.75% w/w)) under magnetic stirring and heating from room temperature to 85 °C. Three cycles of progressive cooling and heating between 85 and 60 °C were then carried out. Step II was an irreversible shock induced by sudden dilution with cold water (70% v/v) to the mixture at 70–72 °C. Slow magnetic stirring was then applied to the suspension for 5 min.

To load the anticancer agent to the oily core of LNCs, FcdiOH was firstly dissolved in Labrafac® under ultrasound at 4% (w/w) for 1.5 h and the resulting lipophilic phase was afterwards mixed with other components as described above. Moreover, in this study, in order to increase the concentration of the drug in the final LNC suspension, the cold water added to the mixture at the step II was decreased from 70% (v/v) for conventional formulations (111 mg of particles per gram of suspension) to 28.5% (v/v) for the concentrated ones (280 mg/g). Final LNC suspensions were filtered through a Minisart 0.2 μm filter (Sartorius) in order to eliminate some unincorporated products.

2.2.2. Fluorescent LNCs

To visualise the LNCs on the brain slides, LNCs were labelled with DiI (emission wavelength = 549 nm; excitation wavelength = 565 nm). The formulation of fluorescent LNCs was similar to that described previously (Garcion et al., 2006). Briefly, DiI was dissolved in acetone at 3 mg/ml and the resulting solution was incorporated in the Labrafac® at proportion of 1:30 (v/v). Acetone solvent was then evaporated before mixing with other components to formulate fluorescent LNCs.

2.2.3. Surface-modified LNCs

DSPE-mPEG2000 was incorporated to the surface of LNCs at the concentration of 10 mM by the post-insertion technique previously described (Morille et al., 2010). Briefly, preformed LNC suspensions and DSPE-mPEG2000 micelles were co-incubated for 2 h at 60 °C. The mixture was vortexed every 15 min and then quenched in an ice bath for 1 min.

2.2.4. Adjustment of the pH and osmolarity of the LNC suspensions

In certain experimental procedures of CED injection, the concentrated LNC suspensions (referred to as crude suspensions) were passed through a PD-10 sephadex column (Amersham Biosciences Europe, Orsay, France) and then concentrated by ultra-filtration with Millipore Amicon 100 kDa centrifugal filter device (Millipore, St. Quentin-Yvelines, France). The osmolarity of the resulting suspensions was then adjusted by adding a 5 M saline solution. Finally, the acidity was neutralised by a 0.1 N NaOH solution in order to obtain adjusted LNCs.

2.3. Characterisation of LNCs

2.3.1. Mean particle size and zeta potential

The LNCs were diluted 1:100 (v/v) in deionised water and the measurements were performed at 25 °C. The LNCs were analysed in triplicate for their mean particle diameter, polydispersity index (PdI) and surface charge using a Malvern Zetasizer® (Nano Serie DTS 1060, Malvern Instruments S.A., Worcestershire, UK).

2.3.2. Osmolarity and pH measurement

The measurement of the pH and osmolarity of the LNC suspensions was performed by using a Consort C561 pH meter

from Avantec (Fisher Bioblock, Scientific) and 5520 Vapro vapour osmometer from Wescor (Logan, Utah, USA), respectively.

2.4. In vivo studies

2.4.1. Animals

Syngeneic Fischer F344 female rats, weighing 160–180 g were obtained from Charles River Laboratories France (L'Arbresle, France). All experiments were performed on 10- to 11-week-old female Fisher rats. Animal care was carried out in strict accordance with French Ministry of Agriculture regulations.

2.4.2. Tumour cell culture

Rat 9L gliosarcoma cells were obtained from the European Collection of Cell Culture (Salisbury, UK, No. 94110705). The cells were cultured at 37 °C in a humidified atmosphere containing 5% CO_2 in Dulbecco's modified Eagle's medium (DMEM) with glucose and L-glutamine (BioWhittaker, Verviers, Belgium) supplied with 10% foetal calf serum (FCS) (BioWhittaker) and 1% antibiotic and antimycotic solution (Sigma, Saint-Quentin Fallavier, France).

2.4.3. Intra-cranial gliosarcoma model

On the day of implantation, a cultured tumour monolayer was detached by using a mixture of trypsin–ethylene diamine tetraacetic acid, then, washed twice with Eagle's minimal essential medium (EMEM) without FCS and antibiotics. Cells were counted, and re-suspended in EMEM to the final concentration of 10^5 9L cells/ml for implantation.

The animals were anaesthetised by intra-peritoneal injection of 1.0 ml/kg of a 1:1 mixture of ketamine (100 mg/ml) (Clorketam®, Vétoquinol, Lure, France) and xylazine (20 mg/ml) (Rompun®, Bayer, Puteaux, France). The incision site was shaved and the head was immobilised in a stereotaxic frame (Lab Standard Stereotaxic; Stoelting, Chicago, IL). A middle scalp incision was made and a burr hole was drilled into the skull using a small dental drill. The cannula coordinates were 1 mm posterior from the bregma, 3 mm lateral from the sagittal suture, and 5 mm below the dura (with the incisor bar set at 0 mm). The 32G needle (Hamilton®), fitted to a 10 μl syringe (Hamilton® glass syringe 700 series RN), was left in place for 5 min and then 10 μl of 10^3 9L cell suspension were injected stereotaxically into the right rat striatum at a flow rate of 2 μl/min. The needle was left in place for 5 additional minutes to avoid expulsion of the suspension from the brain during removal of the syringe, which was withdrawn very slowly (0.5 mm/min). The scalp incision was then closed by using a silk suture (Perma-Hand Seide 3-0, Ethicon).

On Day 6 after 9L cell implantation, rats were injected by means of CED or intra-carotid injection of different LNC formulations.

2.4.4. CED procedure

Tumour-bearing-rats were anaesthetised by an intra-peritoneal injection of 1.5 ml/kg of a 2:1 mixture of ketamine and xylazine. The same procedure of injection as described for cell implantation was applied. The 32G needle (Hamilton®) fitted to a 10 μl Hamilton® syringe was placed in the same coordinates. This syringe was connected to a 100 μl Hamilton syringe 22G (Harvard Apparatus, Les Ulis, France) containing the product through a cannula (CoExTM PE/PVC tubing, Harvard apparatus, Les Ulis, France). Sixty microlitres (60 μl) of LNC suspension were injected by CED which was performed with a pump PHD 2000 infusion (Harvard Apparatus, Les Ulis, France) by controlling a 0.5 μl/min rate for 2 h. The needle was left in place for 5 additional minutes to avoid expulsion of the suspension from the brain during removal of the syringe, which was withdrawn very slowly (0.5 mm/min).

2.4.5. Intra-carotid injection

Tumour-bearing-rats were anaesthetised by an intra-peritoneal injection of 1.0–1.5 ml/kg of a 1:1 solution of ketamine (100 mg/ml) (Clorketam®, Vétoquinol, Lure, France) and xylazine (20 mg/ml) (Rompun®, Bayer, Puteaux, France). The middle neck skin was shaved and incised. The right common carotid (the same side of 9L cell implantation) was exposed and ligated. A PE10 polyethylene catheter (BD Intramedic™ Polyethylene Tubing, Becton Dickinson, USA) was inserted retrogradely through a small arteriotomy. Four hundred microlitres of LNC suspension bolus were injected in into each rat. The catheter was then removed and the carotid artery was ligated.

2.4.6. Side effect monitoring by magnetic resonance imaging and ^{1}H-magnetic resonance spectroscopy

Sixty microlitres of FcdiOH-LNCs were administered by CED (as described in Section 2.4.4) to healthy rats at the same coordinates of tumour implantation. Magnetic resonance imaging (MRI) and ^{1}H magnetic resonance spectroscopy (MRS) were taken on Days 14, 42, 70 and Day 100 after CED injection, to monitor side effects of crude suspension and adjusted suspension of FcdiOH-LNCs with physiological osmolarity and pH values. MRI was performed on a Bruker Avance DRX 300 equipped with a vertical superwide-bore magnet operating at 7 T. Rapid qualitative T2-weighted images were obtained using rapid acquisition with relaxation enhancement (RARE) sequence (TR = 2000 ms; mean echo time (TE) = 31.7 ms; RARE factor = 8; FOV = 3 cm × 3 cm; matrix 128 × 128; nine contiguous slices of 1 mm, eight acquisitions). ^{1}H MRS was performed using a PRESS sequence with water suppression under the following parameters: TR/TE = 1500/11 ms; NEX = 128; voxel size 27 μl (3 mm × 3 mm × 3 mm), as already determined (Lemaire et al., 1999).

2.4.7. Visualisation of fluorescent LNCs in rat brain

For the purpose of tracking the injected LNCs, they were loaded with a fluorescent agent (DiI) instead of an anticancer agent (FcdiOH). DiI-LNCs or DSPE-mPEG2000–DiI-LNCs (400 μl) were administered into tumour-bearing rats through the right common carotid artery. Untreated tumour-bearing rats served as the control group. The rats were euthanised 24 h after injection in a CO_2 chamber. The brain was removed and then snap-frozen in liquid nitrogen-chilled isopentane and stored at −80 °C. Coronal cryosections (14 μm) throughout the tumour zone were performed and recovered on slides. The slides were kept at least 24 h at −20 °C before being processed.

Frozen sections were defrosted at room temperature and rehydrated in Dulbecco's phosphate-buffered saline (DPBS). Sections were fixed in 4% paraformaldehyde and washed with DPBS. Slides were observed under an Axioskop-2 Zeiss fluorescent microscope (Le Peck, France) using a 20× objective. The acquired images were analysed by measuring the fluorescent surface area on the brain tissue slides via integrated morphometry analysis of an inclusive threshold image by use of the Metamorph® software (Roper Scientific, Evry, France). In order to better visualise the nucleus of the tumour cells, some sections were further stained with 1/1000 4′,6-diamidino-2-phenylindole (DAPI) in DPBS for 10 min and then washed with DPBS before mounting.

2.4.8. Efficacy study

The treatment was assessed by CED administration (60 μl, 0.36 mg of FcdiOH/rat), or intra-carotid injection (400 μl, 2.4 mg of FcdiOH/rat) with FcdiOH-LNCs or DSPE-mPEG2000–FcdiOH-LNCs. For CED injection, the osmolarity and pH of the LNC suspensions were adjusted to physiological values whereas the crude suspensions were used for intra-carotid injection. The untreated control group did not receive any treatment. Animals were weighed every

6 days. The animals were sacrificed in a CO_2 chamber when they lost 20% of body weight and/or as soon as they presented seizure, a hunched posture, or haemorrhaging around the eyes, mouth and nose. The death was recorded as if it had occurred on the next day of sacrifice and was represented as the survival time of animals on the Kaplan–Meier curves.

The statistical analysis was estimated from the log-rank test (Mantel-Cox Test) by using StatView software, version 5.0 (SAS institute Inc.). The level of significance was set at $P < 0.05$. The different treatment groups were compared in terms of median and mean survival time (days). The percentage of increase in survival time (% IST) was determined relative to the median and mean survival times of the untreated control group as presented in the following equation:

$$\%\ \text{IST} = \frac{[\text{Median}_T(\text{Mean}_T) - \text{Median}_C(\text{Mean}_C)]}{\text{Median}_C(\text{Mean}_C)}$$

where $\text{Median}_T/\text{Mean}_T$ was the median/mean of survival time of treated group while $\text{Median}_C/\text{Mean}_C$ was the median/mean of survival time of control group.

3. Results and discussion

3.1. Physicochemical properties of LNC suspensions

The physicochemical properties of different types of LNCs are presented in Table 1. All types of LNCs had their average size ranging 44–53 nm with very narrow size dispersion (PdI < 0.08). LNCs were characterised by a slightly negative zeta potential (from −3 to −5 mV), except for DSPE-mPEG2000–FcdiOH-LNCs that presented a zeta potential of bout -22 mV due to the formation of dipoles between PEG molecules and water, as already described (Vonarbourg et al., 2005). The encapsulation of FcdiOH did not affect the average particle size and zeta potential as previously reported (Allard et al., 2008b). This denoted efficient encapsulation of FcdiOH in the oily core of LNCs.

The reduction of cold water added to the final temperature cycle allowed formulating FcdiOH-LNCs at a high drug concentration (6.5 mg of FcdiOH per g of LNC suspension, corresponding to 2% w/w dry weight). This modification did not alter the particle size nor the zeta potential of resulting LNCs compared to the conventional ones (Table 1). However, concentrated blank LNCs as well as FcdiOH-LNCs were hyperosmolar (780.25 ± 7.80 and 773.50 ± 7.05 mmol/kg, respectively) whereas conventional blank LNCs were hypoosmolar (227.50 ± 2.12 mmol/kg). With respect to the suspension acidity, all LNC suspensions presented an acid pH level (pH = 5.3–5.7) and there was no difference between conventional formulations and concentrated ones. After adjustments concerning osmolarity and pH, measurement of particle size and zeta potential showed no changes in these parameters (data not shown).

3.2. Drug delivery by means of the CED technique

3.2.1. Monitoring of side effects by magnetic resonance imaging

In a previous study reporting the treatment of 9L gliosarcoma in rats by CED injection of a concentrated suspension of ^{188}Re-loaded LNCs, the T2-weighted images taken from long-term survivors showed a hyper-intense signal, which was mainly localised in the striatum and persisted until Day 140 of experiments (Allard et al., 2008a). Moreover, ^{1}H MRS showed a decrease in the signal intensity for N-acetylaspartate (NAA) and creatine (Cr). NAA is considered as a valuable marker of brain injury (Demougeot et al., 2001). A decrease in NAA levels detected from MRS suggests neuronal/axonal loss, or compromised neuronal metabolism (Moffett et al., 2007; Schuff et al., 2006). The authors postulated that this lesion was related to internal radiation injury. Unfortunately, these side effects were also observed in a long-term survivor rat that was treated with concentrated suspensions of FcdiOH-LNCs in a previous study concerning tumour-bearing rats (unpublished data).

Therefore, the first set of experiments in the present study was to investigate whether crude FcdiOH-LNCs altered the neuronal metabolism and caused the side effects on healthy rats after a CED administration. T2-weighted images showed that the injection of such a suspension caused a lesion, highlighted by a hyper-intense signal region on the injected hemisphere until Day 70 (Fig. 1A) and characterised by a significant decrease in NAA and Cr intensity of the injected hemisphere as compared to the contralateral hemisphere on proton spectra (Fig. 1B). On the other hand, two high peaks around 0.9–1.5 ppm were observed from the spectrum taken on Day 14 post-injection, which probably corresponded to the peaks of LNC lipids. However, these peaks nearly disappeared by the following reading (Day 42). This underlined the metabolism of LNCs during 6 weeks after injection into the healthy rat striatum. Moreover, these neuronal lesions were also observed in rats receiving blank LNCs with similar hyper-intense signal region on the injected hemisphere on MRI and a considerable decrease in NAA and Cr levels on ^{1}H MRS (figures not shown). Therefore, such side effects could be related to the intrinsic properties of LNC suspensions.

Indeed, administrating a hyperosmotic infusate into the extracellular space produces the movement of water from the intracellular space to the extracellular space, leading to cellular dehydration. This effect potentially induces brain tissue damage, resulting in neurological dysfunction (Petit et al., 2006; Verbalis, 2010). A marked cell volume decrease was observed when incubating cultured human astrocytes with hyperosmotic medium (Anderson et al., 2000). Luh et al. demonstrated that the prolonged exposure of endothelial cells to a hyperosmolar medium (>460 mOsm/L) significantly reduced its viability and function (Luh et al., 1996). Therefore, these previously observed side effects could be linked to the hyperosmolarity of crude LNC suspension which was 2.5-fold higher than physiological osmolarity.

As a consequence, for a safe local administration, we adjusted their osmolarity and pH to physiological conditions as described in Section 2.2.4. Effectively, this formulation did not disturb the normal condition of the brain environment since MRI showed a limited hyper-intense signal zone on the injected hemisphere (Fig. 1C) associated with no difference in NAA and Cr signal intensity between 2 hemispheres on ^{1}H MRS (Fig. 1D).

3.2.2. Efficacy of CED treatment

The survival data from treated tumour-bearing rats are summarised in Table 2 and Kaplan–Meier survival plots are shown in Fig. 2. By applying the criteria for euthanasia of experimental animals, rats were sacrificed when they lost 20% of body weight associated with a high degree of depression. All untreated control rats were sacrificed from Day 22 to Day 26 after 9L cell implantation resulting in a median and mean survival time of 25 days.

The treatment with adjusted FcdiOH-LNCs (60 μl, 0.36 mg/rat) by means of CED significantly increased the median and the mean survival time of animals as compared to the control group (28.5 and 30 days, respectively). On the contrary, treatment with DSPE-mPEG2000–FcdiOH-LNCs in the same dose did not improve the survival of animals as their median remained at 24 days.

The failure of DSPE-mPEG2000–FcdiOH-LNCs treatment could be explained by the abundant presence of PEG, especially with the long chains of PEG at the nanoparticulate surface. Indeed, PEG coating potentially inhibits the internalisation of drug-loaded NPs by tumour cells because it is known to prevent the interactions between the NPs and the tumour cell surface (Hong et al., 1999; Morille et al., 2009). Moreover, the moderated efficacy of FcdiOH

Table 1
Physicochemical properties of LNC suspensions.

		Mean particle size (nm)	Poly-dispersity PdI	Zeta potential (mV)
Conventional formulation	Blank LNCs	49.13 ± 2.18	0.026 ± 0.012	−3.38 ± 0.42
Concentrated formulation	Blank LNCs	49.01 ± 2.18	0.029 ± 0.009	−3.82 ± 0.21
	FcdiOH-LNCs	44.10 ± 0.91	0.025 ± 0.007	−5.05 ± 1.61
	DSPE-mPEG2000–FcdiOH-LNCs	49.08 ± 0.15	0.080 ± 0.006	−21.67 ± 1.10
	DiI-LNCs	49.94 ± 0.22	0.040 ± 0.008	−3.28 ± 0.10
	DSPE-mPEG2000–DiI-LNCs	53.22 ± 1.40	0.041 ± 0.009	−22.50 ± 1.11

by CED administration might be linked to the dose of drug used in this study being not enough high. Indeed, as previously observed, FcdiOH exhibited a cytostatic activity *in vivo* on the intracranial 9L gliosarcoma model in rats in a dose-dependent manner (Allard et al., 2009a). In this previous work, the treatment by CED of FcdiOH dissolved in Labrafac (2.4 mg/rat) at its limited solubility (40 mg/g) gained the median survival time up to 31 days. Unfortunately, some toxic signs were observed in rats treated with drug-free

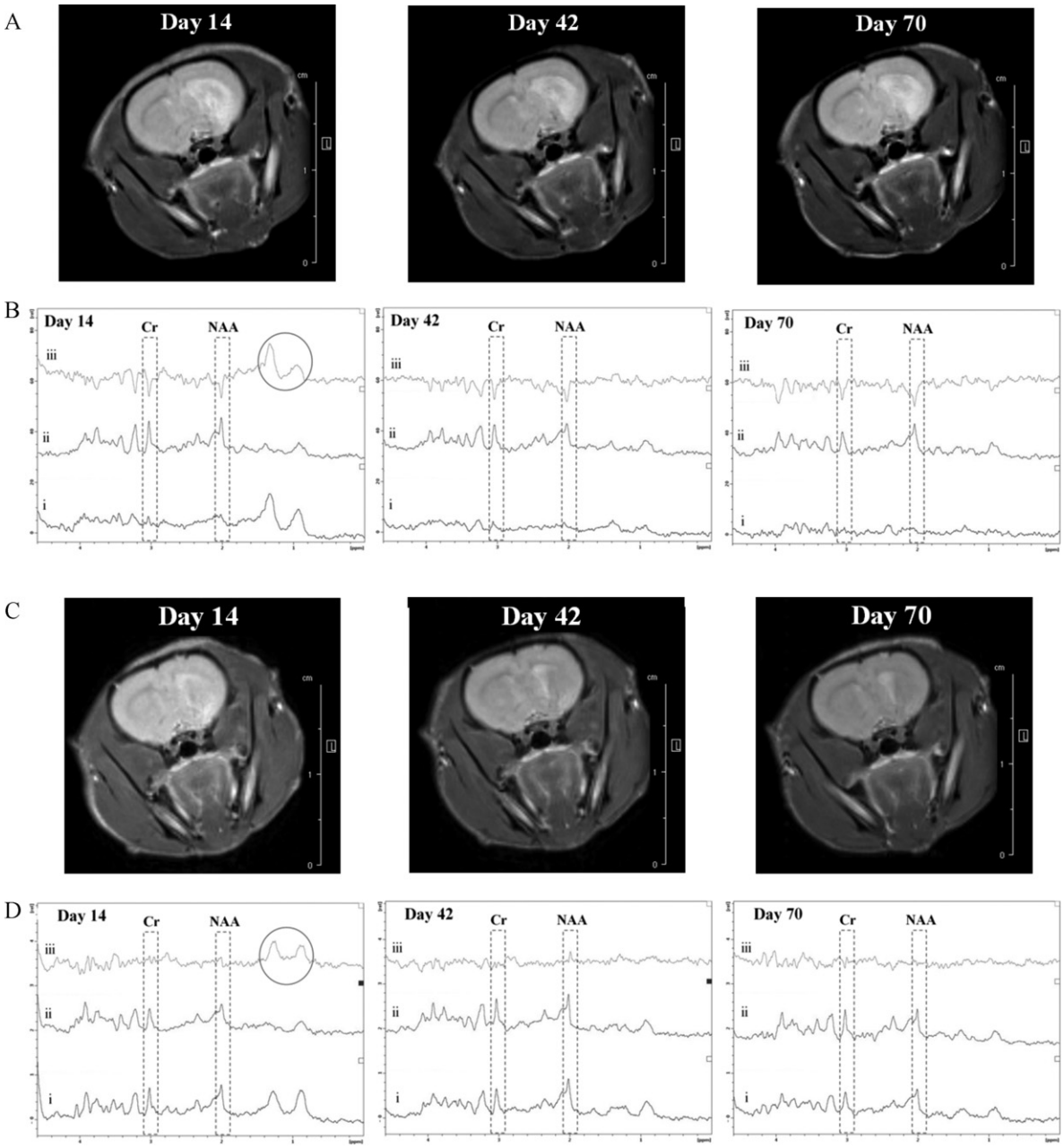

Fig. 1. Representative MRI and ^{1}H MRS taken from healthy rats that received crude FcdiOH-LNCs (A, B) and adjusted FcdiOH-LNCs (C, D). CED injection of crude FcdiOH-LNCs caused a lesion on the injected hemisphere as seen on T2-weighted images (A). The lesions were characterised by a decrease in NAA and Cr intensity (i) as compared to the contralateral hemisphere (ii) that was presented by the difference in signal intensity between 2 hemipheres (iii) on the ^{1}H MRS (B). By adjusting the osmolarity and pH of FcdiOH-LNCs to the physiological values, CED injection of adjusted FcdiOH-LNCs showed a limited hyper-intense signal on the injected hemisphere on T2-weighted images (C) and no difference in NAA and Cr intensity was found in ^{1}H MRS between the 2 hemispheres (D). Spectra taken on Day 14 revealed 2 peaks of LNCs (circle) which disappeared on Day 42.

Table 2
Efficacy of FcdiOH-LNCs and DSPE-mPEG2000–FcdiOH-LNCs in an intracranial 9L gliosarcoma model in Fisher rats (IST: increased survival time).

Administration route (injected dose of FcdiOH)	Treatment	*n*	Survival time (days)			% IST	
			Range	Median	Mean ± SD	Median	Mean
Convection-enhanced delivery (0.36 mg/rat)	FcdiOH-LNCs	8	25–36	28.5	30.13 ± 3.98	14.00	19.90
	DSPE-mPEG2000–FcdiOH-LNCs	8	20–29	24	23.75 ± 3.01	–	–
Intra-carotid (2.4 mg/rat)	FcdiOH-LNCs	7	25–30	27	27.57 ± 2.07	8.00	10.29
	DSPE-mPEG2000–FcdiOH-LNCs	8	26–33	30	29.38 ± 2.50	20.00	17.50
	Untreated control	8	23–27	25	25.13 ± 1.25		–

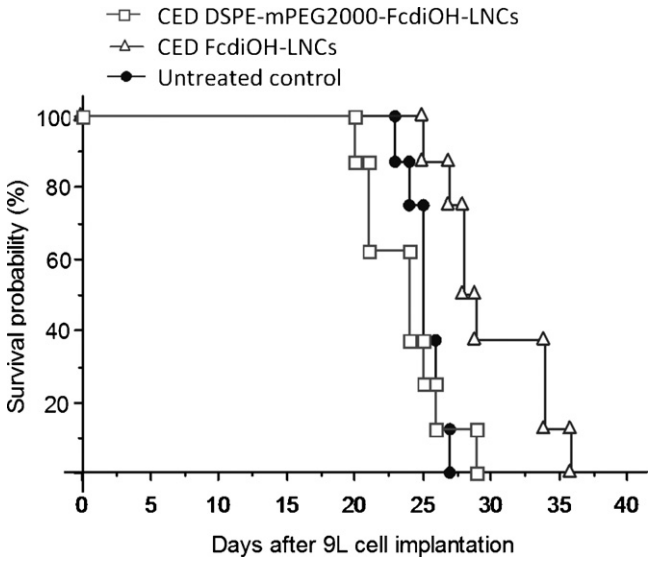

Fig. 2. Kaplan–Meier survival plots for 9L glioma-bearing rats receiving CED injection of DSPE-mPEG2000–FcdiOH-LNCs, FcdiOH-LNCs (60 μl of LNC suspension, corresponding to 0.36 mg of FcdiOH per rat) at Day 6 after cell implantation and untreated animals.

Labrafac showing the limitation of clinical tolerance to Labrafac when infused alone. Thus, taking into consideration the benefit of LNCs in improving intracellular bioavailability (Garcion et al., 2006), these results reveal the necessity of loading FcdiOH into the oily core of LNCs and increasing the volume of the injection as well.

3.3. Drug delivery by intra-carotid injection

Intra-carotid administration can be considered as a regional delivery of drug to the brain that leading to a significant enhancement in drug exposure of the tumoural vasculature (Joshi et al., 2008). In this case, the drug is injected directly into the blood artery and directed towards the brain vasculature before entering peripheral tissues by avoiding the first pass metabolism (Alam et al., 2010). Extensive studies carried out in both experimental animals as well as in humans, have demonstrated benefits of intra-arterial administration in the treatment of brain tumour (Chertok et al., 2010; Figueiredo et al., 2010; Fortin et al., 2005; Fujiwara et al., 1995; Newton, 2006; Newton et al., 2003; Schem and Krossnes, 1995).

In order to test the benefit of this administration route, LNCs were labelled with DiI for the purpose of tracking the injected LNCs. Moreover, this administration route allowed increasing the volume of injection of LNCs from 60 μl for CED injection to 400 μl.

3.4. LNC visualisation in rat brain slices

Fluorescent section images of control rats that did not receive DiI-LNCs showed the auto-fluorescent spots of brain cells which were considered as background noise, and no fluorescence was detected in the brain capillary lumen (Fig. 3A). 24 h after administration of labelled LNCs, including DiI-LNCs or DSPE-PEG-DiI-LNCs by carotid injection, red fluorescence of DiI was observed and could be assigned within the brain tissue (Fig. 3B and C). Especially, in the brain sections of rats receiving DSPE-mPEG2000–DiI-LNCs, the fluorescent spots were largely enhanced throughout the tissues associated with obvious fluorescence of capillary lumen. The mea-

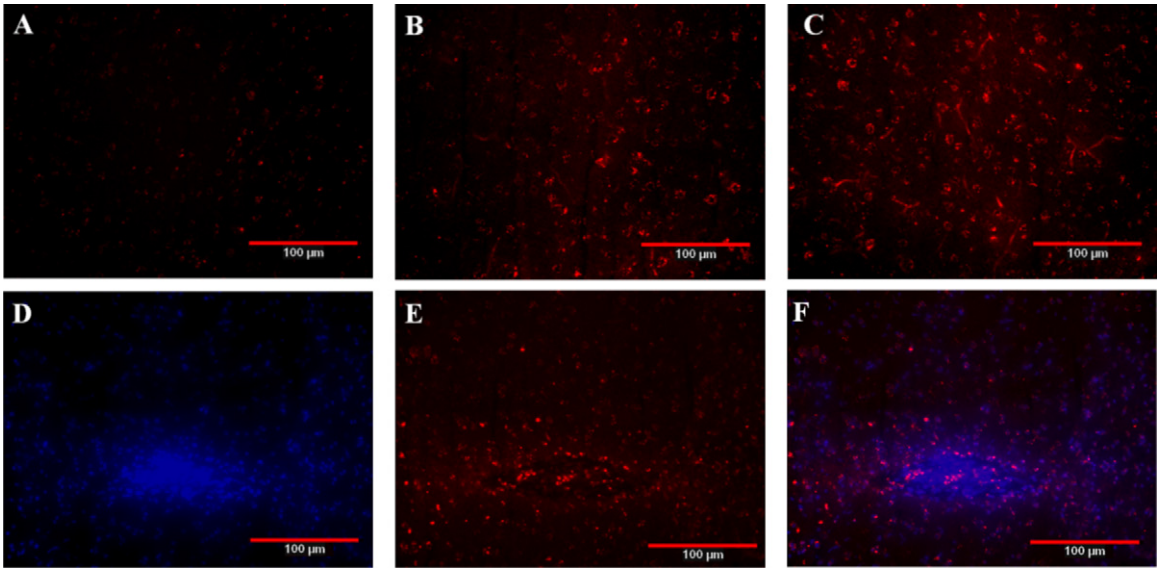

Fig. 3. Section representative image under fluorescent microscope taken from the control tumour-bearing rat (A) and rats receiving an intra-carotid administration of DiI-LNCs (B) or DSPE-mPEG2000–DiI-LNCs (C). The blue-fluorescent DAPI (D) denoted the tumour zone whereas the red fluorescence of DiI (E) showed the distribution of LNCs around the tumour illustrated by the merged image (F).

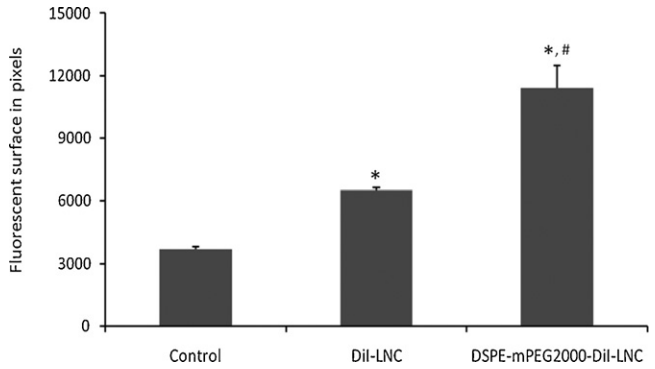

Fig. 4. Semi-quantified presence of LNCs 24 h after administration in the brain slides by measurement of DiI-fluorescent surfaces. * indicates the statistically significant difference in fluorescent surface upon DiI-LNC and DSPE-mPEG2000–DiI-LNC administration from control rats. ≠ indicates the statistically significant difference between DSPE-mPEG2000–DiI-LNC administration and DiI-LNC one.

surements of the fluorescent surface in pixels of inclusive threshold images allowed to semi-quantify the presence of LNCs in the brain slides. As presented in Fig. 4, in comparison with the control, the fluorescent surface significantly increased with DiI-LNC administration and achieved the highest value in the brain slide for rats receiving DSPE-mPEG2000–DiI-LNCs. Indeed, the fluorescent surface measured from these slides was about 1.75-fold higher than that of DiI-LNCs and about 3-fold than that of control.

By labelling cell nuclei with DAPI, the tumour was recognised by blue fluorescence (Fig. 3D) whereas of DiI-labelled nanoparticles was detected by red fluorescence (Fig. 3E). The merged image showed the accumulation of nanoparticles surrounding the tumour zone (Fig. 3F). Consequently, these promising results could potentially lead to an improvement in the therapeutic efficacy of anticancer drug-loaded LNCs on tumour-bearing rats.

3.5. *Efficacy of intra-carotid treatment*

Survival of experimental animals was plotted on the Kaplan–Meier curve as shown in Fig. 5. Results showed that intra-carotid treatment with FcdiOH-LNCs slightly increased the survival

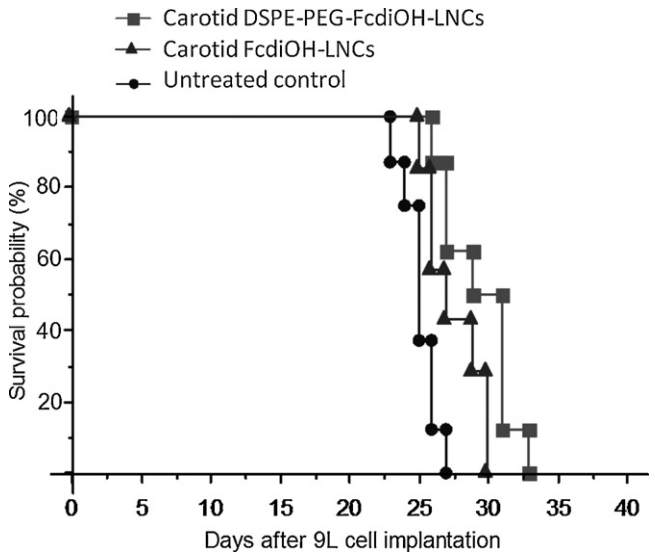

Fig. 5. Kaplan–Meier survival plots for 9L glioma-bearing rats receiving intra-carotid injection of treatment at Day 6 after cell implantation. Survival times were plotted for untreated animals and treated animals with FcdiOH-LNCs or DSPE-mPEG2000–FcdiOH-LNCs (400 μl of LNC suspension, corresponding to 2.4 mg of FcdiOH per rat).

time of treated animals (median = 27 days) and was statistically significant compared to the untreated control group ($P = 0.0177$), and was comparable to treatment by CED injection ($P = 0.3172$) (Fig. 5). Treatment with DSPE-mPEG2000–FcdiOH-LNCs increased the median survival time of rats to 30 days with an IST percentage of 20% ($P = 0.0008$). This result was in agreement with the previously obtained results about the enhanced fluorescent intensity measured from the images of coronal brain slides of rats receiving an intra-carotid injection of DSPE-mPEG2000–DiI-LNCs. This survival time gain is significant and indicates a real treatment benefit as, in clinical trials on human (EORTC/NCIC-protocol), the combination of Temozolomide with focal radiotherapy presents also a 20% IST in comparison to radiotherapy alone (from 12.1 to 14.6 months) (Stupp et al., 2005).

As a well-known characteristic, the coating with long chains of PEG renders nanoparticles 'invisible' to the immune system after injection in the blood that confers stealth properties to PEGylated nanoparticles (Huynh et al., 2010). Thus, PEGylated nanoparticles have more chance to reach tumour tissues and exhibit the intrinsic activity of the entrapped drug. Previously, Morille et al. demonstrated the long-circulating properties of DSPE-mPEG2000–LNCs owing to their weak complement activation and low macrophage uptake associated to an extended half-life in mice as compared to conventional LNCs (Morille et al., 2010).

In addition, for this administration route, crude LNC suspensions were used without the adjustment that was necessary for CED injection. Toxicity was not evaluated in this case as all the components were scattered in the blood flow, which is a different situation from what happens in CED injection. The main purpose for the utility of crude LNCs was to take advantage of the hyperosmolar properties of these suspensions. Indeed, the administration of hypertonic substrates can lead to the opening of tight junctions of the BBB due to the shrinkage of endothelial cells, by which extracellular proteins are disorganised (Alam et al., 2010). Consequently, drug entry takes place in a paracellular fashion and during this state, both diffusion and convection flow across the BBB can be considerably enhanced (Rapoport, 2000). Thus, nanoparticles could potentially reach the brain tumour tissues. The mechanism of brain entry as well as the reversibility and time of junction opening would be essential to determine and will be studied in further experiments.

The remaining matter will be to improve the internalisation of drug into the tumour cells after extravasation. To this end, further optimisation of the LNC surface by attaching active ligands which can specifically recognise tumour cells should be taken into consideration. For example, the covalent coupling of OX26 monoclonal antibodies to LNCs at the end of the PEG molecules leads to the formation of immunonanocapsules which specifically associate *in vitro* to cells over-expressing the transferrin receptor (Beduneau et al., 2008). Indeed, OX26 targets the transferrin receptors which are highly expressed on the cerebral endothelium and also over-expressed on the surface of proliferating cells such as glioma cells (Hall, 1991). This should facilitate the passage of targeting LNCs through the BBB, followed by their internalisation into the tumour cells.

4. Conclusion

To our knowledge, this is the first report involving a neuronal, side-effect study after CED administration of a hyperosmotic infusate. At the same time, intra-arterial injection through the carotid artery was shown to represent a promising route of administration for drug delivery to the brain tumour by giving nanoparticles more chance to cross the BBB. Results revealed the importance of the physicochemical properties of the infusate

versus the brain environment. In each adapted case, the benefit of regional delivery of a drug for brain cancer chemotherapy was evidenced and also confirmed the antitumour efficacy of FcdiOH in an orthotopic 9L gliosarcoma model in rats.

Acknowledgments

The authors would like to thank Pierre Legras (Service Commun d'Animalerie Hospitalo-Universitaire (SCAHU), Angers, France) for his skilful technical support in animal experiments, Pascal Pigeon for the synthesis of FcdiOH and Gerard Jaouen for fruitful discussions. We are also grateful to Jose Hureaux, Laurence Sindji, Frederic Lagarce (Inserm U646, Angers, France) and Florence Franconi (Plateforme d'Ingénierie et d'Analyses Moléculaires (PIAM), Angers, France) for their helpful technical assistance. This work is supported by grants from "La Ligue Nationale Contre le Cancer". Ngoc Trinh Huynh would like to thank the Embassy of France in Vietnam for its Evarist Galoir fellowship.

References

Alam, M.I., Beg, S., Samad, A., Baboota, S., Kohli, K., Ali, J., Ahuja, A., Akbar, M., 2010. Strategy for effective brain drug delivery. Eur. J. Pharm. Sci. 40, 385–403.

Allard, E., Hindre, F., Passirani, C., Lemaire, L., Lepareur, N., Noiret, N., Menei, P., Benoit, J.P., 2008a. 188Re-loaded lipid nanocapsules as a promising radiopharmaceutical carrier for internal radiotherapy of malignant gliomas. Eur. J. Nucl. Med. Mol. Imaging 35, 1838–1846.

Allard, E., Huynh, N.T., Vessieres, A., Pigeon, P., Jaouen, G., Benoit, J.P., Passirani, C., 2009a. Dose effect activity of ferrocifen-loaded lipid nanocapsules on a 9L-glioma model. Int. J. Pharm. 379, 317–323.

Allard, E., Jarnet, D., Vessieres, A., Vinchon-Petit, S., Jaouen, G., Benoit, J.P., Passirani, C., 2010. Local delivery of ferrociphenol lipid nanocapsules followed by external radiotherapy as a synergistic treatment against intracranial 9L glioma xenograft. Pharm. Res. 27, 56–64.

Allard, E., Passirani, C., Benoit, J.P., 2009b. Convection-enhanced delivery of nanocarriers for the treatment of brain tumors. Biomaterials 30, 2302–2318.

Allard, E., Passirani, C., Garcion, E., Pigeon, P., Vessieres, A., Jaouen, G., Benoit, J.P., 2008b. Lipid nanocapsules loaded with an organometallic tamoxifen derivative as a novel drug–carrier system for experimental malignant gliomas. J. Control Release 130, 146–153.

Anderson, A.W., Xie, J., Pizzonia, J., Bronen, R.A., Spencer, D.D., Gore, J.C., 2000. Effects of cell volume fraction changes on apparent diffusion in human cells. Mag. Reson. Imaging 18, 689–695.

Beduneau, A., Hindre, F., Clavreul, A., Leroux, J.C., Saulnier, P., Benoit, J.P., 2008. Brain targeting using novel lipid nanovectors. J. Control Release 126, 44–49.

Bobo, R.H., Laske, D.W., Akbasak, A., Morrison, P.F., Dedrick, R.L., Oldfield, E.H., 1994. Convection-enhanced delivery of macromolecules in the brain. Proc. Natl. Acad. Sci. U.S.A. 91, 2076–2080.

Chertok, B., David, A.E., Yang, V.C., 2010. Polyethyleneimine-modified iron oxide nanoparticles for brain tumor drug delivery using magnetic targeting and intracarotid administration. Biomaterials 31, 6317–6324.

Demougeot, C., Garnier, P., Mossiat, C., Bertrand, N., Giroud, M., Beley, A., Marie, C., 2001. N-acetylaspartate, a marker of both cellular dysfunction and neuronal loss: its relevance to studies of acute brain injury. J. Neurochem. 77, 408–415.

Figueiredo, E.G, Faria, J.W., Teixeira, M.J., 2010. Treatment of recurrent glioblastoma with intra-arterial BCNU [1,3-bis (2-chloroethyl)-1-nitrosourea]. Arq. Neuropsiquiatr. 68, 778–782.

Fortin, D., Desjardins, A., Benko, A., Niyonsega, T., Boudrias, M., 2005. Enhanced chemotherapy delivery by intraarterial infusion and blood–brain barrier disruption in malignant brain tumors: the Sherbrooke experience. Cancer 103, 2606–2615.

Fujiwara, T., Matsumoto, Y., Honma, Y., Kuyama, H., Nagao, S., Ohkawa, M., 1995. A comparison of intraarterial carboplatin and ACNU for the treatment of gliomas. Surg. Neurol. 44, 145–150.

Garcion, E., Lamprecht, A., Heurtault, B., Paillard, A., Aubert-Pouessel, A., Denizot, B., Menei, P., Benoit, J.P., 2006. A new generation of anticancer, drug-loaded, colloidal vectors reverses multidrug resistance in glioma and reduces tumor progression in rats. Mol. Cancer Ther. 5, 1710–1722.

Grossman, S.A., Batara, J.F., 2004. Current management of glioblastoma multiforme. Semin. Oncol. 31, 635–644.

Hall, W.A., 1991. Transferrin receptor on glioblastoma multiforme. J. Neurosurg. 74, 313–314.

Heurtault, B., Saulnier, P., Pech, B., Proust, J.E., Benoit, J.P., 2002. A novel phase inversion-based process for the preparation of lipid nanocarriers. Pharm. Res. 19, 875–880.

Hillard, E., Vessieres, A., Thouin, L., Jaouen, G., Amatore, C., 2005. Ferrocene-mediated proton-coupled electron transfer in a series of ferrocifen-type breast-cancer drug candidates. Angew. Chem. – Int. Ed. 45, 285–290.

Hong, R.L., Huang, C.J., Tseng, Y.L., Pang, V.F., Chen, S.T., Liu, J.J., Chang, F.H., 1999. Direct comparison of liposomal doxorubicin with or without polyethylene glycol coating in C-26 tumor-bearing mice: is surface coating with polyethylene glycol beneficial? Clin. Cancer Res. 5, 3645–3652.

Huynh, N.T., Passirani, C., Saulnier, P., Benoit, J.P., 2009. Lipid nanocapsules: a new platform for nanomedicine. Int. J. Pharm. 379, 201–209.

Huynh, N.T., Roger, E., Lautram, N., Benoit, J.P., Passirani, C., 2010. The rise and rise of stealth nanocarriers for cancer therapy: passive versus active targeting. Nanomedicine (Lond) 5, 1415–1433.

Jaouen, G., Top, S., Vessieres, A., Alberto, R., 2000a. New paradigms for synthetic pathways inspired by bioorganometallic chemistry. J. Organomet. Chem. 600, 23–36.

Jaouen, G., Top, S., Vessières, A., Leclercq, G., Quivy, J., Jin, L., Croisy, A., 2000b. The first organometallic antioestrogens and their antiproliferative effects. C. R.Acad. Sci. – Ser. IIc: Chem. 3, 89–93.

Joshi, S., Meyers, P.M., Ornstein, E., 2008. Intracarotid delivery of drugs: the potential and the pitfalls. Anesthesiology 109, 543–564.

Lemaire, L., Franconi, F., Lejeune, J.J., Jallet, P., Richomme, P., 1999. Improving the detection of low concentration metabolites in magnetic resonance spectroscopy by digital filtering. Med. Biol. Eng. Comput. 37, 244–246.

Louis, D.N., Ohgaki, H., Wiestler, O.D., Cavenee, W.K., Burger, P.C., Jouvet, A., Scheithauer, B.W., Kleihues, P., 2007. The 2007 WHO classification of tumours of the central nervous system. Acta Neuropathol. 114, 97–109.

Luh, E.H., Shackford, S.R., Shatos, M.A., Pietropaoli, J.A., 1996. The effects of hyperosmolarity on the viability and function of endothelial cells. J. Surg. Res. 60, 122–128.

Moffett, J.R., Ross, B., Arun, P., Madhavarao, C.N., Namboodiri, A.M.A., 2007. N-acetylaspartate in the CNS: from neurodiagnostics to neurobiology. Prog. Neurobiol. 81, 89–131.

Morille, M., Montier, T., Legras, P., Carmoy, N., Brodin, P., Pitard, B., Benoit, J.P., Passirani, C., 2010. Long-circulating DNA lipid nanocapsules as new vector for passive tumor targeting. Biomaterials 31, 321–329.

Morille, M., Passirani, C., Letrou-Bonneval, E., Benoit, J.P., Pitard, B., 2009. Galactosylated DNA lipid nanocapsules for efficient hepatocyte targeting. Int. J. Pharm. 379, 293–300.

Newton, H.B., 2006. Intra-arterial chemotherapy. In: Herbert, B.N., Faan, M.D. (Eds.), Handbook of Brain Tumor Chemotherapy. , first ed. Academic Press, San Diego, pp. 247–261.

Newton, H.B., Slivka, M.A., Volpi, C., Bourekas, E.C., Christoforidis, G.A., Baujan, M.A., Slone, W., Chakeres, D.W., 2003. Intra-arterial carboplatin and intravenous etoposide for the treatment of metastatic brain tumors. J. Neurooncol. 61, 35–44.

Pardridge, W.M., 2005. The blood–brain barrier: bottleneck in brain drug development. NeuroRx 2, 3–14.

Parkin, D.M., Bray, F., Ferlay, J., Pisani, P., 2005. Global Cancer Statistics, 2002. CA: Cancer J. Clin. 55, 74–108.

Petit, L., Masson, F., Cottenceau, V., Sztark, F., 2006. Hypernatrémie contrôlée. Ann. Fr. Anesth. Reanim. 25, 828–837.

Rapoport, S.I., 2000. Osmotic opening of the blood-brain barrier: principles, mechanism, and therapeutic applications. Cell. Mol. Neurobiol. 20, 217–230.

Schem, B.C., Krossnes, B.K., 1995. Enhancement of ACNU treatment of the BT4an rat glioma by local brain hyperthermia and intra-arterial drug administration. Eur. J. Cancer 31, 1869–1874.

Schuff, N., Meyerhoff, D.J., Mueller, S., Chao, L., Sacrey, D.T., Laxer, K., Weiner, M.W., 2006. N-acetylaspartate as a marker of neuronal injury in neurodegenerative disease. Adv. Exp. Med. Biol. 576, 241–262, discussion 361–243.

Segal, M.B., 2000. The choroid plexuses and the barriers between the blood and the cerebrospinal fluid. Cell. Mol. Neurobiol. 20, 183–196.

Stupp, R., Mason, W.P., van den Bent, M.J., Weller, M., Fisher, B., Taphoorn, M.J., Belanger, K., Brandes, A.A., Marosi, C., Bogdahn, U., et al., 2005. Radiotherapy plus concomitant and adjuvant temozolomide for glioblastoma. N. Engl. J. Med. 352, 987–996.

Top, S., Vessieres, A., Leclercq, G., Quivy, J., Tang, J., Vaissermann, J., Huche, M., Jaouen, G., 2003. Synthesis, biochemical properties and molecular modelling studies of organometallic specific estrogen receptor modulators (SERMs), the ferrocifens and hydroxyferrocifens: evidence for an antiproliferative effect of hydroxyferrocifens on both hormone-dependent and hormone-independent breast cancer cell lines. Chemistry 9, 5223–5236.

Verbalis, J.G., 2010. Brain volume regulation in response to changes in osmolality. Neuroscience 168, 862–870.

Vessieres, A., Top, S., Pigeon, P., Hillard, E., Boubeker, L., Spera, D., Jaouen, G., 2005. Modification of the estrogenic properties of diphenols by the incorporation of ferrocene. Generation of antiproliferative effects in vitro. J. Med. Chem. 48, 3937–3940.

Vinchon-Petit, S., Jarnet, D., Paillard, A., Benoit, J.P., Garcion, E., Menei, P., 2010. In vivo evaluation of intracellular drug-nanocarriers infused into intracranial tumours by convection-enhanced delivery: distribution and radiosensitisation efficacy. J. Neurooncol. 97, 195–205.

Vonarbourg, A., Saulnier, P., Passirani, C., Benoit, J.P., 2005. Electrokinetic properties of noncharged lipid nanocapsules: influence of the dipolar distribution at the interface. Electrophoresis 26, 2066–2075.